Received: 21 September 2017 | Revised: 26 November 2017 | Accepted: 30 November 2017
DOI: 10.1002/ardp.201700294

FULL PAPER

DPhG ARCH PHARM
Archiv der Pharmazie

Design, synthesis, and pharmacological evaluation of fluorinated azoles as anti-tubercular agents

Somnath Gholap[1] | Macchindra Tambe[1] | Laxman Nawale[2] | Dhiman Sarkar[2] | Jaiprakash Sangshetti[3] | Manoj Damale[4]

[1] Postgraduate Department of Chemistry and Research Centre, Padmashri Vikhe Patil College, Pravaranagar, A/P-Loni kd, Tal.-Rahata, Ahmadnagar, India

[2] Division of Organic Chemistry, Combichem-Bioresource Centre, National Chemical Laboratory, Pune, India

[3] Y. B. Chavan College of Pharmacy, Aurangabad, India

[4] Bhagwan College of Pharmacy, Aurangabad, India

Correspondence
Dr. Somnath Gholap, Postgraduate Department of Chemistry and Research Centre, Padmashri Vikhe Patil College, Pravaranagar, A/P-Loni kd, Tal.-Rahata, Dist.-Ahmadnagar, Pin-413713 (MS), India.
Email: ssgholap2002@gmail.com

Abstract

Design, synthesis, and biological screening of 2,2-dimethyl-2,3-dihydrobenzofuran tethered 1,3,4-oxadiazole derivatives as anti-tubercular agents were described. The synthesis of the target compounds was conducted by a series of reaction schemes. All the synthesized compounds were characterized by IR, ^{1}H NMR, ^{13}C NMR, and mass spectrometry. The therapeutic potential of the synthesized compounds was confirmed by molecular docking studies. Among the synthesized compounds, **12a**, **12c**, **12d**, **12e**, **12g**, and **12j** were found to be more active against non-replicating than against replicating cultures of *Mycobacterium tuberculosis* H37Ra *ex vivo* and *in vitro*. These compounds exhibit minimum inhibitory concentration (MIC) values in the range of 2.31–23.91 μg/mL. The cytotoxicity study was conducted against the cell lines THP-1, A549 and PANC-1, and the compounds were observed to be non-toxic to host cells. Molecular docking was conducted with InhA (FabI/ENR) and suggested the antimycobacterial potential of the synthesized compounds. The investigation presented here was found to be adventitious for the development of new therapeutic agents against *Mycobacterium* infection.

KEYWORDS
1,3,4-oxadiazole, 2,2-dimethyl-2,3-dihydrobenzofuran, anti-tubercular agents, cytotoxicity, molecular docking

1 | INTRODUCTION

Tuberculosis is a leading infectious bacterial disease caused by *Mycobacterium tuberculosis*.[1,2] At present, approximately 30 *Mycobacterium* genus are responsible to cause human diseases among the bacterial genus.[3] In particular, human immune deficiency virus (HIV) infected persons are more susceptible to *Mycobacterium* infections.[4] Nowadays, multi-drug resistant (MDR) tuberculosis is more common,[5] as well as continuing problem of the extremely drug resistant (XDR) or totally drug resistant (TDR) forms of tuberculosis.[6,7] The available first line anti-TB chemotherapy required nearly 6 months to 1 year to cure the infection completely with complex medication course.[8,9] The treatment of multi drug resistant tuberculosis suffered by toxic, poorly tolerated, and less effective medication for long-time.[10] Hence, there is urgent need to develop effective drug candidate against *M. tuberculosis*.

The 1,3,4-oxadiazole derivatives are well known nitrogen heterocycles possessing broad spectrum of bioactivities and found to be good bioisosters of amide and ester functionalities.[11] The structural features of the oxadiazole core displayed interesting H-bond acceptor properties, which improves lipophilicity profile and adequate ADME properties.[12] Some of the 1,3,4-oxadiazole derivatives such as **A**, **B**, **C**,

and **D** was reported as good anti-TB activity with MIC 0.78 to 1.6 μg/mL, respectively[13] and zibotentan (**E**) was found to be potent anticancer agent[14] (Figure 1).

Moreover, 1,3,4-oxadiazole derivatives exhibit diverse biological profile such as anti-HIV,[15] antimalarial,[16] analgesic,[17] antiinflammatory,[18] anticonvulsant,[19] and as lipid peroxidase inhibitors.[20] Interestingly, the constrained analogue of isopropyl phenyl ether such as 2,2-dimethyl-2,3-dihydrobenzofuran has been found in zatosetron (**F**) as 5-HT3 antagonist[21] and derivative G as serotonin 2C agonist[22] (Figure 2). In the view of the biocompatibility and biological potential of 1,3,4-oxadiazole as well as 2,2-dimethyl-2,3-dihydrobenzofuran core, herein, we have reported the design, synthesis, molecular docking, and biological screening of some new 1,3,4-oxadiazole based 2,3-dihydrobenzofuran derivatives (Scheme 1). The targeted compounds were designed in such a way that the 1,3,4-oxadiazole and 2,2-dimethyl-2,3-dihydrobenzofuran core will be conserved together with incorporation of the groups as H-bond acceptors and H-bond donors at particular sites[23,24] (Figure 3).

2 | RESULTS AND DISCUSSION

In continuation to our ongoing research on the synthesis of biologically active oxadiazole derivatives,[25–31] herein, we have reported the synthesis of novel structurally diverse 1,3,4-oxadiazole possessing 2,2-dimethyl-2,3-dihydrobenzofuran core (**12a–j**) (Table 1) and evaluated their biological potential. The structure of the synthesized compounds was confirmed by their characterization data obtained by IR, NMR, and mass spectral analysis study.

2.1 | Chemistry

The target compounds **12a–j** were synthesized as depicted in Scheme 1. The starting compound 4-acetamido-2-hydroxy benzoic acid (**2**) was synthesized by *N*-acetylation of 2-hydroxy-4-amino-benzoic acid (**1**). The *N*-acetylated derivative on subsequent nitration gaves 4-acetamido-2-hydroxy-5-nitrobenzoic acid (**3**). The esterification of 4-acetamido-2-hydroxy-5-nitrobenzoic acid followed by deprotection of *N*-acetyl was achieved in a one-pot reaction with methanol and catalytic amount of sulfuric acid furnished to methyl 4-amino-2-hydroxy-5-nitrobenzoate (**4**). The alkylation of compound **4** with 3-chloro-2-methyl propene in *N*,*N*-dimethyl formamide at 70°C gave methyl 2-(2-methyl allyloxy)-4-amino-5-nitrobenzoate (**5**). The Claisen rearrangement of intermediate compound **5** was conducted with anhydrous $AlCl_3$ in dichloromethane to afforded methyl-4-amino-2,3-dihydro-2,2-dimethyl-5-nitrobenzofuran-7-carboxylate (**6**). Sandmayer reaction of compound **6** was furnished compound methyl-2,3-dihydro-4-iodo-2,2-dimethyl-5-nitrobenzofuran-7-carboxylate 7, which was further hydrolyzed using LiOH to afforded 2,3-dihydro-4-iodo-2,2-dimethyl-5-nitrobenzofuran-7-carboxylic acid (**8**) followed by treatment with oxalyl chloride and 4-trifluoromethyl phenyl hydrazide to give 4-iodo-5-nitro-2,2-dimethyl-*N*-[4-(trifluoromethyl)benzoyl]-2,3-dihydrobenzofuran-7-carbohydrazide (**9**). The *N*-benzoyl hydrazide (**9**) on cyclization with $POCl_3$ afforded 2-[4-(trifluoromethyl) phenyl-5-(2,3-dihydro-4-iodo-2,2-dimethyl-5-nitrobenzofuran-7-yl]-1,3,4 oxadiazole (**10**). The compound **10** on reduction with Fe followed by the reaction of pivolyl chloride in THF at room temperature afforded *N*-(7-(5-(4-(trifluoromethyl)phenyl)-1,3,4-oxadiazol-2-yl)-2,3-dihydro-4-iodo-2,2-dimethyl benzofuran-5-yl)pivalamide (**11**). The compound **11** on Sonogashira coupling[32–37] with terminal alkynes using $PdCl_2(PPh_3)_2$ at 80°C furnished target compounds **12a–j** in a good to excellent yield (70–85%) (Scheme 1, Figure 4, Table 1). The purification of all synthesized compounds was conducted by column chromatography using methanol/dichloromethane (4%) as eluent system. As representative IR spectrum of **12a** showed absorption at 3426 cm^{-1} due to the presence of amide (-NH stretching), absorption at 2211 cm^{-1} due to

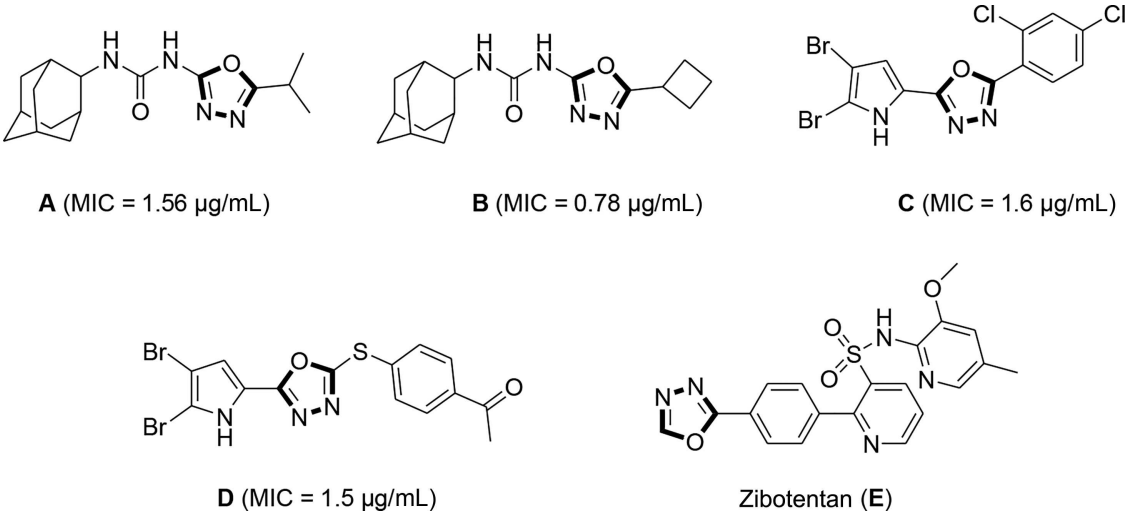

FIGURE 1 Potentially active 1,3,4-oxadiazole derivatives

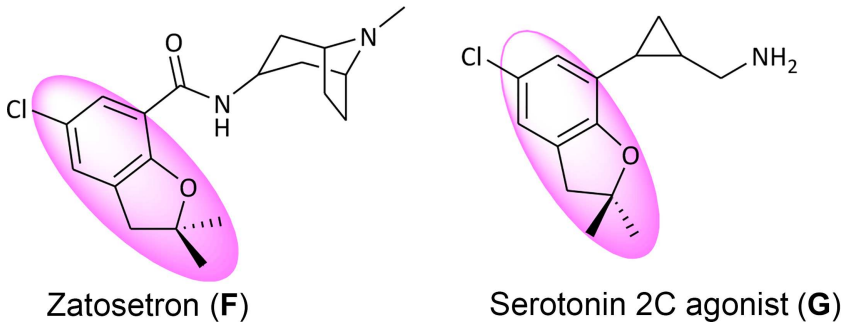

FIGURE 2 Bioactive 2,2-dimethyl-2,3-dihydrobenzofuran derivatives

C≡C, at 1678 cm^{-1} due to C═O stretching of amide group, peak at 1494 cm^{-1} due to C—F streching, absorption at 1324 cm^{-1} due to C═N. The NMR spectrum of **12a**, ^{1}H NMR (300 MHz, DMSO-d_6): δ 1.28 (s, 9H), 1.58 (s, 6H), 3.28 (s, 2H), 7.48 (d, *J* = 7.6 Hz, 3H), 7.55 (d, *J* = 7.6 Hz, 2H), 7.92 (s, 1H), 8.03 (d, *J* = 7.8 Hz, 2H), 8.30 (d, *J* = 7.8 Hz, 2H), 9.15 (s, 1H, exchangeable with D_2O); ^{13}C NMR (125.7 MHz, $CDCl_3$): δ 27.8, 28.5, 40.2, 42.9, 88.4, 89.6, 90.7, 106.1, 117.6, 120.8, 126.1, 127.3, 127.5, 127.6, 128.7, 128.9, 129.7, 130.2, 131.7, 131.8, 132.0, 132.2, 135.9, 153.6, 162.9, 176.2. The mass spectrum of **12a** (M.F. $C_{32}O_3N_3F_3H_{28}$, M.W. = 559.57) showed molecular ion peak at *m/z* = 560.03 $(M+H)^+$.

2.2 | Biological activity

2.2.1 | Anti-tubercular activity studies

The synthesized compounds **12a–j** were screened for their *ex vivo/in vitro* antitubercular activity against *M. tuberculosis* H_{37}Ra and *M. bovis* BCG with concentrations of 30, 10, and 3 μg/mL using XRMA (H37Ra) and nitrate reductase model (BCG) as per protocols reported in literature.[38–40] The percentage inhibition at above concentrations was calculated and collected in Table S1 (Supporting Information). The compounds **12c**, **12g**, and **12j** exhibited higher

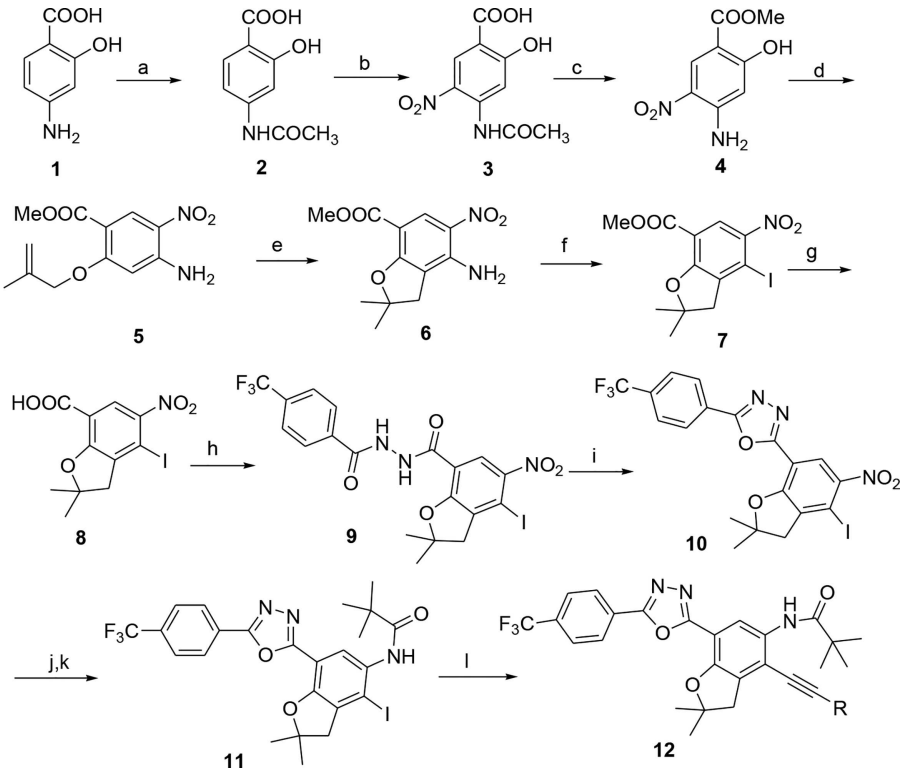

SCHEME 1 Synthesis of 1,3,4-oxadiazole derivatives. Reagents and conditions: (a) Ac_2O, EtOH, reflux, 3 h, 88%. (b) $NaNO_3$, TFA, 0°C, 3 h, 70%. (c) Methanol, H_2SO_4, reflux, 24 h, 97%. (d) 3-Chloro-2-methyl propene, K_2CO_3, DMF, 70°C, 5 h, 80%. (e) Anhy. $AlCl_3$, CH_2Cl_2, −78 to 25°C, 24 h, 83%. (f) Conc. HCl, $NaNO_2$, KI, 0°C, 3 h, 90%. (g) LiOH, THF, H_2O, 2 h, 93.90%. (h) CH_2Cl_2, oxalyl chloride, 25°C, 2 h, 85%. (i) 4-Trifluoromethyl phenyl hydrazide, TEA, THF, 0°C, (ii) $POCl_3$, reflux, 10 h, 74.1%. (j) Fe, MeOH, conc. HCl, 1 h, 80%. (k) Pivolyl chloride, TEA, THF, 25°C, 76.8%. (l) Acetylene, $PdCl_2(PPh_3)_2$, TBAF, DMSO, 80°C, 3 h, 70–85%

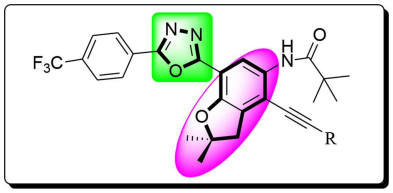

FIGURE 3 Molecular structure of designed compound

anti-mycobacterial potency (inhibiting >90% of mycobacterial growth at 30 µg/mL with rifampicin as reference drug). In general, the newly synthesized compounds showed excellent selectivity toward *M. tuberculosis* $H_{37}Ra$ and *M. bovis* BCG strains. The anti-tubercular data obtained showed growth inhibition MTB and BCG can be imparted by the introduction of a hydroxyprop-1-ynyl group at 4-position of **12j**. Most of the compounds were more active against non-replicating than replicating cultures of *M. tuberculosis* H37Ra by *ex vivo* as well as by *in vitro*. The percentage inhibition at above concentrations was calculated and collected in Table S1. Three of the compounds viz. **12c**, **12g**, and **12j** showed MIC in the range of 2.31–23.91 µg/mL proving their anti-tubercular potential (Table 2).

2.2.2 | Cytotoxicity studies

The cytotoxicity study of the synthesized compounds **12c**, **12g**, **12j**, **12a**, **12d**, and **12e** was conducted as per reported procedures[40] using various concentrations as 100, 50, 25, 12.5, 6.25, 3.125, 1.5625, and 0.7813 µg/mL against three human cancer cell lines (THP-1, A549, and PANC-1)[40] (Table 3). In order to interpret the cytotoxicity results, the synthesized compounds and indication of their specific inhibition against MTB, the compounds **12c**, **12g**, and **12j** were evaluated for the determination of GI_{50}/GI_{90} values. It has been found that all of the compounds showed very low cytotoxicity at GI_{50} <90; >100 µM against THP-1 and >147 µM against A549 and PANC-1 cells. The selectivity of **12a**, **12c**, **12d**, **12e**, **12g**, and **12j** toward human cell lines against MTB and BCG is described in terms of the selectivity index (Table 4).

The selectivity index (SI) reflects the concentration of the compound at which it is active against mycobacteria *M. bovis* BCG but is not toxic toward host cells. The higher selectivity index value, the compound can be used as a therapeutic agent. The synthesized compound "**12j**" showed a very high SI index, which is actually good inhibitor of *M. tuberculosis* and *M. bovis* BCG. Although the selectivity index of rifampicin is very high, it is important to consider the significance of this study with respect to the developing resistance

TABLE 1 Synthesis of 1,3,4-oxadiazole bearing 2,2-dimethyl-2,3-dihydrobenzofuran derivatives (**12a–j**)

Entry	R	Compound (12)	Time (h)	Yield (%)[a,b,c]	M.P. (°C)
1.	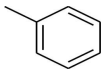	**12a**	2.5	85	188–189
2.	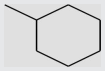	**12b**	2.0	82	171–172
3.	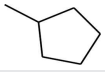	**12c**	2.5	80	172–173
4.		**12d**	2.3	82	176–177
5.	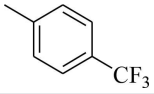	**12e**	4.0	75	190–191
6.	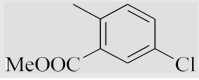	**12f**	5.5	78	198–199
7.	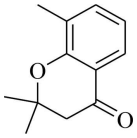	**12g**	6.3	70	212–213
8.		**12h**	4.5	75	126–127
9.		**12i**	4.5	70	132–133
10.		**12j**	4.0	75	182–183

[a]Isolated yields of the products after purification.
[b]Yields of the products in final step.
[c]All synthesized compounds were characterized by IR, ^{1}H-NMR, ^{13}C-NMR and mass spectral data.

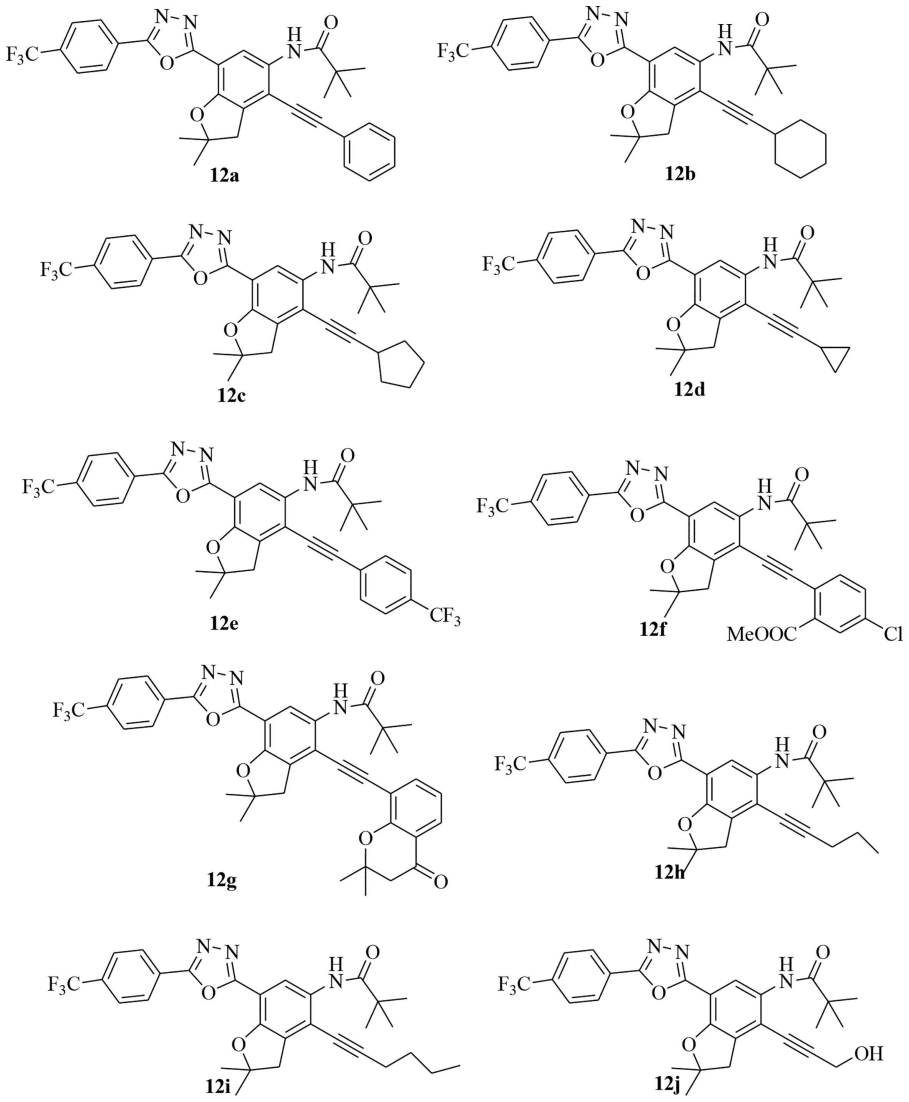

FIGURE 4 Structures of synthesized compounds

among microorganisms against available antibiotics. According to a study of Hartkoorn et al.,[41] on the drug susceptibility of TB, antimycobacterial activity was considered to be specific when the selectivity index was >10. In the current report, compound **12j** exhibited highest selectivity index of >10, indicating its potential as an antitubercular agent, and thus it should be investigated further.

2.2.3 | Antibacterial screening study

The anti-tubercular screening results strengthen the fact that the synthesized compounds will exhibit antimicrobial activity. Therefore, the antibacterial screening of the synthesized compounds was conducted against four bacteria strains (Gram-negative strains: *E. coli*, *S. aureus*; Gram-positive strains: *P. aeruginosa* and *B. subtilis*).[40] The compounds **12a**, **12c**, **12d**, **12e**, **12g**, and **12j** showed higher specificity toward MTB as these compounds showed nil anti-bacterial activity up to 100 μg/mL. (Table 5) [40].

2.3 | Molecular docking study

Furthermore, the molecular docking study supports the InhA inhibition, binding mode, and identification of the structural features of the active molecules from series of synthesized compounds. As InhA (FabI/ENR) is an enoyl-ACP reductase as one of the key enzymes of *M. tuberculosis* implicated in the biosynthesis of cell wall constituents such as mycolic acids, the docking study was conducted with the mycobacterial enoylreductase (InhA) (PDB code 4TZK).[42–44]* [*The complex X-ray crystal structures of enoyl-ACP reductase with inhibitors pyrrolidine carboxamide (PDC) for *Mycobacterium* was retrieved from the RCSB protein data bank (http://www.rcsb.org/pdb) and used for the docking study. The molecular docking study has been performed with Tripos SYBYL X 2. 2.1 program.[45]

In the previous studies of synthesis and biological evaluation of 1,3,4-oxadiazole, derivative has been reported for inhibition of mycobacterial enoylreductase (InhA) which made a firm basis for selection of this enzyme as the potential target. The molecular docking

TABLE 2 Experimentally determined anti-mycobacterial activity (*ex vivo*/*in vitro*) of the key compounds

	IC_{50} and IC_{90} values (μM) of compounds with SD (±) values		
	M. tuberculosis H37Ra (ATCC 25177)	*M. tuberculosis* H37Ra (ATCC 25177)	*M. bovis* BCG (ATCC 35743)
	Ex vivo (dormant)	*In vitro* (dormant)	*In vitro* (dormant)
Compound	IC_{90}	IC_{90}	IC_{90}
12a	>53.67	>53.67	>53.67
12c	40.24 ± 1.05	43.39 ± 0.29	24.46 ± 1.28
12d	>57.25	>57.25	>57.25
12e	>47.77	>47.77	>47.77
12g	19.22 ± 0.6	21.22 ± 1.11	19.73 ± 1.55
12j	4.50 ± 0.69	5.67 ± 0.89	5.40 ± 0.92
Rifampicin	0.972 ± 0.04	0.911 ± 0.01	1.009 ± 0.02

SD (±), standard deviation.

study will act as a key indicator to understand the basis of molecular inhibition of enoyl-ACP reductase activity.[46–49] It was also helped in correlation of *in vivo* and *in vitro* activity of the newly synthesized compounds.

The computational (theoretical) prediction data from the molecular docking study was found to be replicated in the results of experimental anti-tubercular activity. All the compounds **12a**, **12b**, **12c**, **12d**, **12e**, **12f**, and **12j** were successfully docked into the active site of target enzyme mycobacterial enoylreductase (InhA/FabI/ENR) and it has been observed that they have varying degrees of affinity to the active site residues. Majority of the amino acids present in the active site cavity such as glycine, alanine, leucine, isoleucine, proline, phenylalanine, tyrosine, methonine, arginine, lysine, aspartic acid, and glutamic acid. Depending on the physicochemical properties, these are non-polar or hydrophobic, polar charged, non-charged, negatively charged, and positively charged amino acid residues. The detailed molecular interactions study between active site amino acid residue and components of the molecule was carried out to understand the thermodynamic stability of different 1,3,4-oxadiazole bearing 2,2-dimethyl-2,3-dihydrobenzofuran derivatives which also provide information about binding modes observed within the active site cavity. The theoretical values of the molecular docking study are presented in Table 6.

To represent the details of docking score following terms is used as Total score as Total Docking Score, Crash Score as degree of inappropriate penetration by the ligand into the protein and of interpenetration between ligand atoms that are separated by rotatable bonds of compounds and Polar Score gives an idea about the contribution of the polar non-hydrogen bonding interactions to the total score is shown in Table 6. The value of Total Score (inhibition constant-logK_i) provides an indication of how potent an inhibitor is. Higher the value for the total score (inhibition constant-logK_i), more is the potency of inhibitor.[50] The high value of total score indicates potency of highest value **12j** which indicate that it is most active among the six docked molecules. The compound binds and inhibits with a total docking score of 7.3242, Crash Score of −3.1839 which indicate degree of inappropriate penetration by the ligand into the protein and of interpenetration between ligand atoms that are separated by rotatable bonds and Polar Score of 1.0449 contributions of the polar non-hydrogen bonding interactions to the total score.

The detailed analysis of the binding interactions and binding pose of **12j** showed that it is stabilized within the active site of InhA through an extensive network of favorable non-covalent interactions such as π interaction, π–π T-shaped interaction, alkyl interaction, and π-alkyl interactions. As a part of non-covalent interactions, fluorine atom of tri-fluoromethyl interacts with amino acids such as Asp42 and Agr43 forms H–F interactions with distance of 2.81, 3.14, and 275 Å, respectively. π–π T-shaped interactions Phe41 with aryl ring of distance 4.67 Å. The hydrophobic amino acid Ile16 forms π and π-alkyl interactions with aryl, oxadiazole, and methyl groups of benzofuryl ring with a distance of 4.66, 4.33, and 4.89 Å, respectively. The amino acid Ala198 forms π and π-alkyl interactions with dihydrobenzofuryl group and methyl substituent of

TABLE 3 Cytotoxicity of selected compounds in three human cancer cell lines after 48 h of exposure

	Cytotoxic profile of key compounds against human cancer cell lines with SD (±) values					
	A549		PANC-1		THP-1	
Compound ID	GI_{50}	GI_{90}	GI_{50}	GI_{90}	GI_{50}	GI_{90}
12a	>178.89	>178.89	>178.89	>178.89	>178.89	>178.89
12c	>181.49	>181.49	>181.49	>181.49	101.00 ± 1.09	>181.49
12d	>190.84	>190.84	>190.84	>190.84	>190.84	>190.84
12e	>159.24	>159.24	>159.24	>159.24	>159.24	>159.24
12g	>151.98	>151.98	>151.98	>151.98	112.67 ± 1.03	>151.98
12j	193.37 ± 0.87	>194.93	147.54 ± 0.97	>194.93	169.90 ± 0.76	>194.93
[c]Paclitaxel	0.004 ± 0.00012	0.083 ± 0.09	0.150 ± 0.17	6.693 ± 0.15	0.006 ± 0.00014	0.088 ± 0.2

SD (±), standard deviation.

TABLE 4 Selectivity index (SI) of selected key compounds on three human cell lines against *M. tuberculosis* H37Ra (*ex vivo*/*in vitro*) and *M. bovis* BCG (*in vitro*)

	SI on A549			SI on PANC-1			SI on HeLa		
	Ex vivo	*In vitro*	*In vitro*	*Ex vivo*	*In vitro*	*In vitro*	*Ex vivo*	*In vitro*	*In vitro*
	H37Ra	H37Ra	BCG	H37Ra	H37Ra	BCG	H37Ra	H37Ra	BCG
Entry	SI against dormant stage of *M. tuberculosis* H37Ra and *M. bovis* BCG								
12a	3	3	3	3	0	3	3	3	3
12c	5	4	7	5	0	7	3	2	4
12d	3	3	3	3	0	3	3	3	3
12e	3	3	3	3	0	3	3	3	3
12g	8	7	8	8	1	8	6	5	6
12j	43	34	36	33	11	27	38	30	31
Rifampicin	125	133	120	125	167	120	125	133	120

dihydrobenzofuryl group with atomic distance of 3.27 and 4.33 Å, respectively. The hydrophobic amino acids such as Ile21 and polar charged amino acid form π-alkyl interactions with acetyl methyl hydrogen of distance of 4.87, 3.99, and 4.59 Å, respectively, as shown in Figure 5.

2.4 | The physicochemical and pharmacokinetic parameters prediction studies

The physicochemical and pharmacokinetic parameters prediction was conducted by calculation and analysis of various physical descriptors and pharmaceutical relevant properties for ADMET prediction by using FAFDrugs2 and data is summarized in Table 7. The drug likeness was predicted by analyzing absorption, distribution, metabolism, and elimination (ADME) parameters based on Lipinski's rule of five and its variants.[51] This approach has been widely used as a filter for substances that would likely be further developed for drug design programs who has assumptions as molecular weight (<500), partition coefficient LogP (<5), number of hydrogen bond donor (<10), number of hydrogen bond acceptor (<5), number of rotatable bonds (<10), total polar surface area (<75 $Å^2$). The % ABS: percentage absorption also predicated using formula ABS = 109 − (0.345 × TPSA). To increase the rate of drug likeness predication Veber suggested some variations like molecular weight can be considered above 500 Da, total polar surface area (<150 $Å^2$), partition coefficient LogP (<5.6). All the compounds showed significant values for the various parameters analyzed and showed good drug-like characteristics based on Lipinski's rule of five and its variants that characterized that these agents as likely orally active.[52] The values of % ABS, polar surface area (PSA), n-HBA, and n-HBD for synthesized compounds **12a**, **12c**, **12d**, **12e**, **12g**, and **12j** indicated good oral bioavailability as depicted in Table 7. The *in silco* assessment of all the synthetic compounds showed that they have very good pharmacokinetic properties which was reflected in their physicochemical values and which ultimately contributing for pharmacological properties of these molecules.

TABLE 5 Antibacterial activity against *E. coli*, *Pseudomonas aeruginosa*, *Staphylococcus aureus*, *Bacillus subtilis*

	In vitro anti-bacterial activity of selected key compounds			
	E. coli	*P. aeruginosa*	*S. aureus*	*B. subtilis*
	Gram-negative		Gram-positive	
Entry	IC_{90} (μM)	IC_{90} (μM)	IC_{90} (μM)	IC_{90} (μM)
12a	177.17 ± 2.53	175.56 ± 6.96	151.06 ± 5.24	166.78 ± 6.36
12c	>181.49	>181.49	>181.49	>181.49
12d	188.40 ± 4.66	186.68 ± 4.95	185.76 ± 3.46	184.85 ± 2.30
12e	>159.24	>159.24	>159.24	>159.24
12g	>151.98	>151.98	142.26 ± 4.46	136.44 ± 4.57
12j	>194.93	>194.93	>194.93	>194.93
Ampicillin	4.18 ± 0.72	12.48 ± 1.88	2.86 ± 0.98	29.54 ± 1.25
Kanamycin	3.34 ± 1.62	1.01 ± 0.50	>61.92	2.79 ± 0.19

SD (±), standard deviation.

TABLE 6 Experimentally determined anti-mycobacterial activity (*ex vivo*/*in vitro*) of the key compounds and molecular docking details

	IC_{50} and IC_{90} values (μM) of compounds with CI (±) values			Molecular docking score		
	M. tuberculosis H37Ra (ATCC 25177)	*M. tuberculosis* H37Ra (ATCC 25177)	*M. bovis* BCG (ATCC 35743)			
	Ex vivo (dormant)	*In vitro* (dormant)	*In vitro* (dormant)			
Entry	IC_{90}	IC_{90}	IC_{90}	Total score (−logK_i)	Crash score	Polar score
12a	>53.67	>53.67	>53.67	4.1411	−5.1433	0.3551
12c	40.24 ± 1.05	43.39 ± 0.29	24.46 ± 1.28	4.7562	−1.674	0.5103
12d	>57.25	>57.25	>57.25	7.2417	−4.581	0.0028
12e	>47.77	>47.77	>47.77	4.5721	−2.0919	0.4167
12g	19.22 ± 0.6	21.22 ± 1.11	19.73 ± 1.55	5.3567	−4.5584	0.0001
12j	4.50 ± 0.69	5.67 ± 0.89	5.40 ± 0.92	7.3242	−3.1839	1.0449
Rifampicin	0.972 ± 0.04	0.911 ± 0.01	1.009 ± 0.02	NA	NA	NA

Total score, total docking score; Crash, degree of inappropriate penetration by the ligand into the protein and of interpenetration between ligand atoms that are separated by rotable bonds; Polar, contribution of the polar non-hydrogen bonding interactions to the total score.

2.5 | The biotransformation prediction

The biotransformation prediction was performed by MetaPrint2D-React, a metabolic product predictor server developed by Unilever Cambridge, Center for Molecular Science Informatics, University of Cambridge, UK. It is online tool that predicts fate of xenobiotics metabolism through data-mining and statistical analysis of known metabolic transformations reported in scientific literature.[53–54] The MetaPrint2D data is generated through processing of the transformations found in the Symyx Metabolite database previously known as MDL, for each transformation, the differences between the structures of the reactant. In order to make predictions of on the drug molecule, each atom environment is calculated and Symyx Metabolite database mining is done to search similar environment.

As based on the interest of the study, only Phase I additions (defined as the addition of a single oxygen atom; covering hydroxylation, oxidation, and epoxidation), and eliminations (e.g., dealkylation, ester, and amide hydrolysis) are engaged.[55] In addition, the atom neighboring the added oxygen is highlighted as a reaction center. The most active anti-tubercular compounds **12j** (Figure 5) and **12c** (Figure 6) are analyzed for metabolic product prediction. The plot of MetaPrint2D-React shows possible site of metabolism of individual atom neither indicated by Normalized Occurrence Ratio (NOR) values. The higher NOR value indicates site frequently undergoes through particular metabolism phase I metabolic reactions.[56,57] The NOR ratio for **12j** was observed as Red 0.66 ≤ NOR ≤ 1.00, Orange 0.33 ≤ NOR < 0.66, Green 0.15 ≤ NOR < 0.33, White (no color) 0.00 ≤ NOR < 0.15, and Gray little/no data. The NOR ratio for **12c** was observed as Red 0.66 ≤ NOR ≤ 1.00, Yellow 0.33 ≤ NOR < 0.66, Green 0.15 ≤ NOR < 0.33, and White (no color) 0.00 ≤ NOR < 0.15. The NOR values and atoms marks for **12j** indicate that >C$(CH_3)_2$ group of dihydrobenzofuran and −CF_3 of phenyl ring mostly undergoes through the hydroxylation reactions, whereas, in

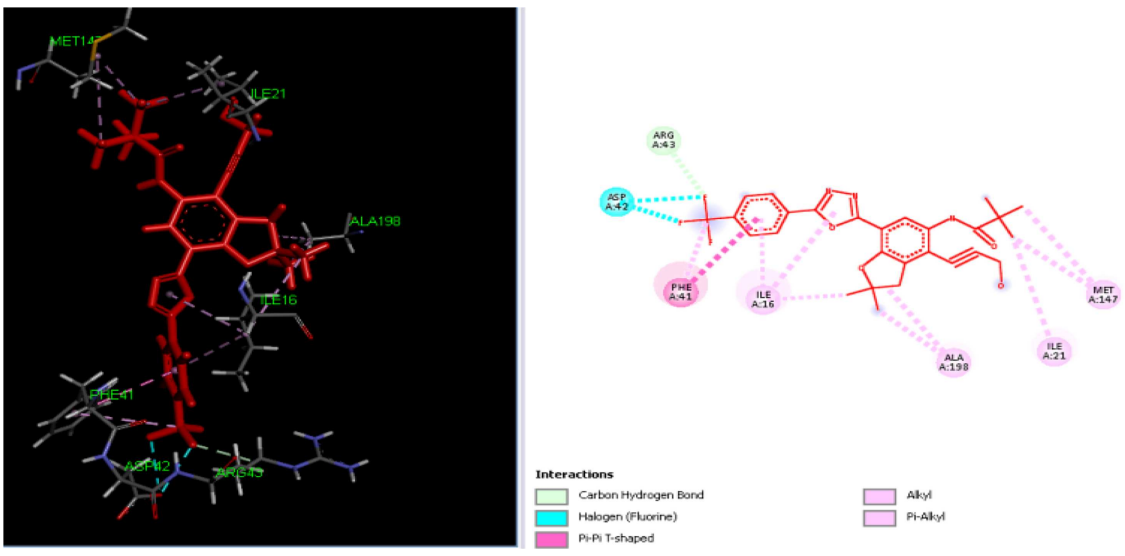

FIGURE 5 Binding pose and molecular interactions of **12j** into the active site of InhA

TABLE 7 Pharmacokinetic parameters important for agents to have good oral bioavailability of synthesized compounds

ID	MW	LogP	PSA	% ABS	n-RotB	HBD	HBA	Toxicity
12a	559.57823	7.5933	77.25	81.6535	5	1	5	Non toxic
12c	551.59929	7.7352	77.25	81.6535	5	1	5	Non toxic
12d	523.54613	6.955	77.25	81.6535	5	1	5	Non toxic
12e	627.5762	8.6121	77.25	81.6535	6	1	5	Non toxic
12g	657.67817	8.3371	103.55	72.3433	5	1	7	Non toxic
12j	513.5082	5.5373	97.48	74.49208	5	2	6	Non toxic

MW, molecular weight; LogP, logarithm of partition coefficient of compound between *n*-octanol and water; PSA, polar surface area; n-RotBond, number of rotatable bonds; HBA, hydrogen bond acceptors; and HBD, hydrogen bond donor.

12d dimethyl group of dihydrobenzofuran undergoes hydroxylation and $-CF_3$ also undergoes the hydroxylation reaction. Above observations indicated that some atoms in skeleton of the target compounds were less prone to metabolic deactivation marked by grey color (Figures 7 and 8).

3 | CONCLUSION

In conclusion, a series of structurally diverse 2,2-dimethyl-2,3-dihydrobenzofuran based 1,3,4-oxadiazole derivatives were successfully synthesized and characterized by spectral data. The synthesized compounds were screened for *ex vivo* and *in vitro* anti-tubercular studies. The tested compounds **12c**, **12g**, and **12j** were found to have good anti-tubercular activity against *M. tuberculosis* H37Ra, *M. bovis* BCG strains. The compound **12j** shows excellent anti-tubercular potential (MIC < 6 μM) for *ex vivo* and *in vitro* anti-tubercular studies. The experimental, molecular docking, pharmacokinetics/druglike properties and metabolic pathway prediction values of synthesized agents provide a potential pharmacophore for further drug development process.

4 | EXPERIMENTAL

4.1 | Chemistry

4.1.1 | General methods

All the reagents used during the study were purchased from Aldrich and Spectro-Chem. Solvents were dried and redistilled before use. Melting points were recorded on Digital Electro thermal Melting point apparatus (VEEGO, VMP-DS) and are uncorrected. Reaction monitoring was conducted using thin layer chromatography (TLC) using pre-coated silica gel 60 F_{254} plates with layer thickness 0.25 nm purchased from Merck Ltd. TLC plates were visualized under ultraviolet light at 254 nm wavelength. IR spectra were recorded on KBr discs on Shimazdzu 470 IR spectrophotometer. ^{1}H-NMR was recorded on Varian-NMR mercury 300 MHz spectrometer in DMSO-d_6 using TMS as an internal standard. Chemical shifts values (δ) are expressed as parts per million (ppm). Mass spectra were recorded on a Varian MAT 311 A at 70 eV.

IR and NMR spectra as well as the InChI codes of the investigated compounds together with some biological activity data are provided as Supporting Information.

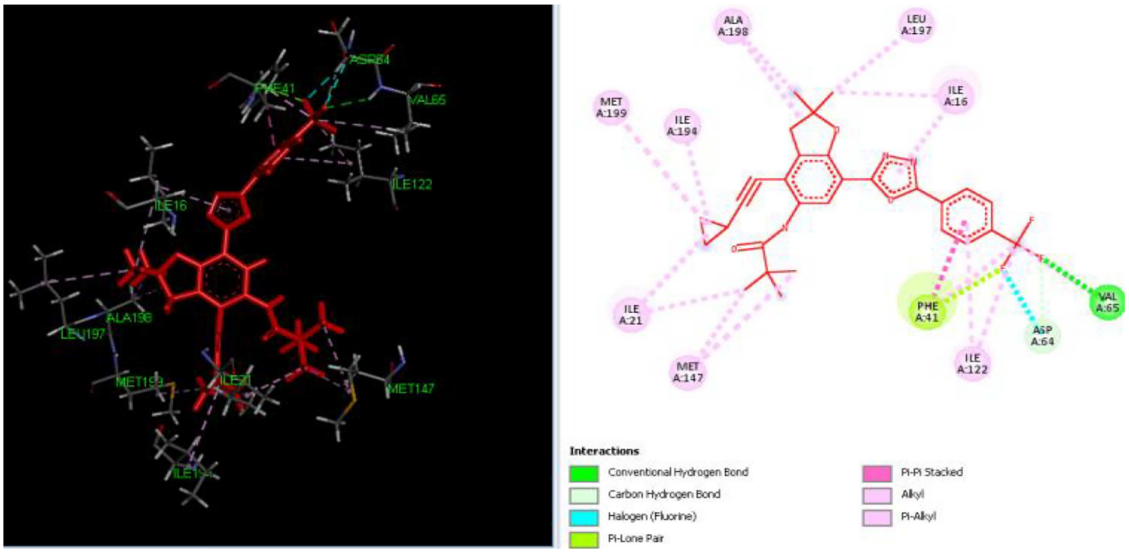

FIGURE 6 Binding pose and molecular interactions of **12d** into the active site of InhA

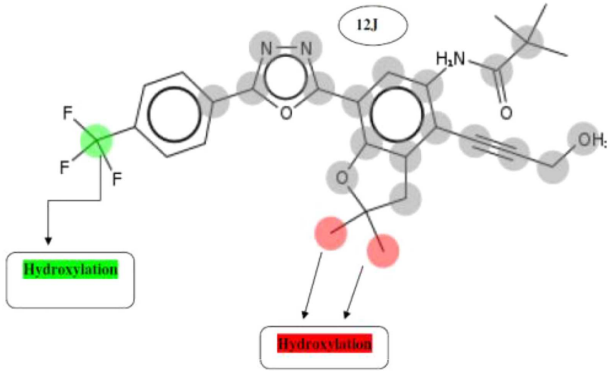

FIGURE 7 Metabolic deactivation pathways by MetaPrint-2D React of compound **12j**

Synthesis of 4-acetamido-2-hydroxy benzoic acid (2)

To a mixture of 4-amino salicylic acid (50 g, 0.32 mol) in ethanol, acetic anhydride (43.30 mL, 0.42 mol) was added. The reaction mixture was stirred at 45–50°C for 3 h. After completion of reaction (as indicated by TLC), reaction mixture was cooled and poured on ice. The product precipitated which was then filtered and collected to afford **2** as white solid (56 g), yield = 88%, mp = 216–217°C. ^{1}H NMR (300 MHz, DMSO-d_6): δ 2.06 (s, 3H, CH_3), 7.02 (d, J = 6.9 Hz, 1H, Ar-H), 7.33 (s, 1H, Ar-H), 7.68 (d, J = 8.7 Hz, 1H, Ar-H), 10.20 (s, 1H, -NHCO-), 11.40 (s, 1H exchangeable with D_2O, Ar-OH), 13.00 (s, 1H exchangeable with D_2O, -COOH); M.F. = $C_9O_4NH_9$ (MW = 195.22) m/z 196 $(M+H)^+$.

Synthesis of 4-acetamido-2-hydroxy-5-nitrobenzoic acid (3)

To a mixture of 4-acetamido-2-hydroxy benzoic acid (56 g, 0.287 mol) in trifluoroacetic acid (560 mL), sodium nitrate (26.84 g, 315 mol) was added slowly and reaction mixture was cooled to 0°C. After completion of reaction (by TLC), reaction mixture was poured on ice. The yellow solid separated was filtered to afford **3** (45 g), yield = 70%, mp = 202–204°C. ^{1}H NMR (300 MHz, DMSO-d_6): δ 2.16 (s, 3H, -CH_3), 7.64 (s, 1H, Ar-H), 8.44 (s, 1H, Ar-H), 10.43 (s, 1H, Ar-OH); M.F. = $C_9O_6N_2H_8$ (MW = 240.12) m/z 241 $(M+H)^+$.

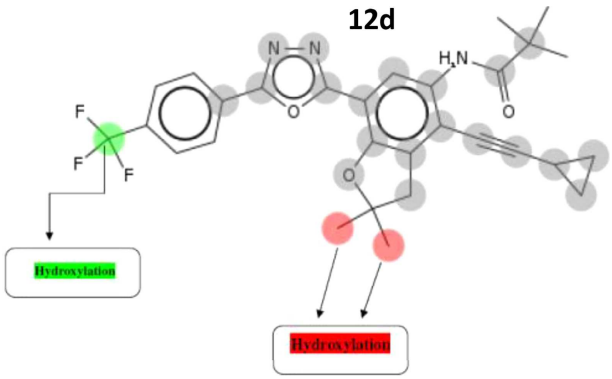

FIGURE 8 Metabolic deactivation pathways by MetaPrint-2D React of compound **12d**

Synthesis of methyl 4-amino-2-hydroxy-5-nitrobenzoate (4)

To a mixture of 4-acetamido-2-hydroxy-5-nitrobenzoic acid (44 g, 0.287 mol) in methanol (440 mL), conc. H_2SO_4 (176 mL) was slowly added. Reaction mixture was stirred at 65°C for 24 h. After completion of reaction (as indicated by TLC), reaction mixture was cooled and poured on ice. The product precipitated was filtered to afford **4** as yellow solid (40 g), yield = 97%; mp = 184–186°C; ^{1}H NMR (300 MHz, DMSO-d_6): δ 3.84 (s, 3H, -CH_3), 6.36 (s, 1H, Ar-H), 7.96 (s, 2H, exchangeable with D_2O, Ar-NH_2), 8.52 (s, 1H, Ar-H), 10.92 (s, 1H, exchangeable with D_2O, Ar-OH); M.F. = $C_8O_5N_2H_8$ (MW = 212.11) m/z 213.05 $(M+H)^+$.

Synthesis of methyl 2-(2-methyl allyloxy)-4-amino-5-nitrobenzoate (5)

To a mixture of methyl-4-amino-2-hydroxy-5-nitrobenzoate (**4**) (15 g, 0.0707 mol) in dry DMF (90 mL), K_2CO_3 (17.5 g, 0.127 mol) was added. Reaction mixture was stirred at 80°C for 1 h. To the above mixture, 3-chloro-2-methyl prop-1-ene (11.4 g, 0.127 mol) was added slowly and a reaction mixture was further stirred at 80°C for 3 h. After completion of reaction (by TLC), reaction mixture was cooled and poured on ice. The product precipitated was filtered and collected to afford **5** as yellow solid (15 g), yield = 80 %; mp = 148–149°C; ^{1}H NMR (300 MHz, DMSO-d_6): δ 1.79 (s, 3H,-CH_3), 3.75 (s, 3H, -OCH_3), 4.47 (s, 2H, -NH_2), 4.98 (s, 1H), 5.19 (s, 1H), 6.50 (s, 1H, Ar-H), 7.82 (s, 2H, -CH_2-), 8.50 (s, 1H, Ar-H); M.F. = $C_{12}O_5N_2H_{15}$ (MW = 266.11) m/z 267.10 $(M+H)^+$.

Synthesis of methyl-4-amino-2,3-dihydro-2,2-dimethyl-5-nitrobenzofuran-7-carboxylate (6)

To a mixture of methyl-2-(2-methylallyloxy)-4-amino-5-nitrobenzoate (**5**) (15 g, 0.056 mol) in dry dichloromethane (90 mL), anhydrous $AlCl_3$ (1.5 g, 0.0112 mol) was added slowly at −78°C. Reaction mixture was further stirred at −78°C for 1 h. Reaction mixture gradually allowed to stand at room temperature for 24 h. After completion of reaction (as indicated by TLC), reaction mixture was cooled and poured on ice. The product precipitated was filtered and recrystallized from ethyl acetate to give **6** as a yellow solid (12.5 g), yield = 83%; mp = 173–174°C. ^{1}H NMR (300 MHz, DMSO-d_6): δ 1.47 (s, 6H), 2.87 (s, 2H), 3.75 (s, 3H), 7.49 (s, 2H, exchangeable with D_2O), 8.51 (s, 1H); M.F. = $C_{12}O_5N_2H_{14}$ (MW = 266.11), m/z 267 $(M+H)^+$.

Synthesis of methyl-2,3-dihydro-4-iodo-2,2-dimethyl-5-nitrobenzofuran-7-carboxylate (7)

A mixture of methyl-4-amino-2,3-dihydro-2,2-dimethyl-5-nitrobenzofuran-7-carboxylate (12 g, 0.0451 mol) and conc. HCl (96 mL, 8 vol) was cooled at 0°C for 30 min. To this reaction mixture, aqueous solution of sodium nitrite (4.66 g, 0.0676 mol in water 10 mL) was added slowly using dropping funnel. The temperature of reaction mixture was maintained as 0°C. The solution of KI (11.22 g, 0.067 mol in 20 mL water) was added slowly at 0°C during 1 h. After completion of reaction, the reaction mixture was extracted by EtOAC, washed with water and separated. The organic layer was dried over anhydrous sodium sulphate and solvent was removed under reduced pressure followed by recrystallization using diethyl ether to give **7** as a yellow

solid (15.2 g), yield = 89.41%; mp = 138–139°C. ^{1}H NMR (300 MHz, DMSO-d_6): δ 1.51 (s, 6H), 3.10 (s, 2H), 3.81 (s, 3H), 8.24 (s, 1H); M.F. = $C_{12}O_5NIH_{12}$ (MW = 377.21) *m/z* 378 $(M+H)^+$.

Synthesis of 2,3-dihydro-4-iodo-2,2-dimethyl-5-nitrobenzofuran-7-carboxylic acid (8)

To a mixture of methyl-2,3-dihydro-4-iodo-2,2-dimethyl-5-nitrobenzofuran-7-carboxylate (**7**) (15 g, 0.039 mol) in THF, LiOH (1.83 g, 0.079 mol) was added at 25°C. The reaction mixture was stirred at 25°C for 1 h. After completion of reaction, THF was removed under reduced pressure and reaction mixture was acidified by dil. HCl, solid precipitated out was filtered and collected to afford **8** as a yellow solid (13.5 g); yield = 93.90%; mp = 120–121°C; ^{1}H NMR (DMSO-d_6, 300 MHz): δ 1.50 (s, 6H), 3.09 (s, 2H), 8.23 (s, 1H); M.F. = $C_{11}O_5NIH_{10}$ (MW = 363.11) *m/z* 364 $(M+H)^+$.

Synthesis of 4-iodo-5-nitro-2,2-dimethyl-*N*-[4-(trifluoromethyl)-benzoyl]-2,3-dihydrobenzofuran-7-carbohydrazide (9)

To the reaction mixture of 2,3-dihydro-4-iodo-2,2-dimethyl-5-nitrobenzofuran-7-carboxylic acid (**8**) (13.5 g, 0.037 mol) in dry dichloromethane (70 mL), oxalyl chloride (11.82 mL, 0.074 mol) was added at 25°C followed by addition of 2–3 drops of DMF. The reaction mixture was stirred at 25°C for 1–2 h. After completion of reaction, the solvent was removed under reduced pressure and residue was mixed with dichloromethane and cooled to 0°C. Triethylamine (8 mL, 0.074 mol) and 4-trifluoromethyl phenyl hydrazide (7.5 g, 0.037 mol) was added at 0°C. Reaction mixture was stirred at 0°C for 2 h. After completion of reaction (by TLC), reaction mixture was cooled and poured on ice. Solid separated was filtered to afford **9** as a brown yellow solid (15 g); mp = 154–155°C. ^{1}H NMR (300 MHz, DMSO-d_6): δ 1.58 (s, 6H), 3.17 (s, 2H), 7.92 (d, *J* = 8.4 Hz, 2H), 8.12 (d, *J* = 8.4 Hz, 2H), 8.26 (s, 1H), 10.16 (s, 1H), 10.88 (s, 1H); M.F. = $C_{19}O_5N_3IF_3H_{15}$ (MW = 548) *m/z* 549.13 $(M+H)^+$.

Synthesis of 2-[4-(trifluoromethyl)phenyl-5-(2,3dihydro-4-iodo-2,2-dimethyl-5-nitrobenzofuran-7-yl]-1,3,4-oxadiazole (10)

A mixture of 4-iodo-5-nitro-2,2-dimethyl-*N*-[4-(trifluoromethyl)benzoyl]-2,3-dihydrobenzofuran-7-carbohydrazide (**9**) (15 g) and $POCl_3$ (50 mL) was heated under reflux for 10 h. After completion of reaction $POCl_3$ was distilled out completely, residue was slowly added in ice cold water, solid precipitated collected to afford compound **10** as a brown solid, yield = 74%; mp = 187–188°C. ^{1}H NMR (300 MHz, DMSO-d_6): δ 1.60 (s, 6H), 3.20 (s, 2H), 8.01 (d, *J* = 7.8 Hz, 2H), 8.30 (d, *J* = 7.8 Hz, 2H), 8.51 (s, 1H); M.F. = $C_{19}O_4N_3IF_3H_{13}$ (MW = 530.11) *m/z* 531 $(M+H)^+$.

Synthesis of *N*-(7-(5-(4-(trifluoromethyl)phenyl)-1,3,4-oxadiazol-2-yl)-2,3-dihydro-4-iodo-2,2-dimethyl benzofuran-5-yl)pivalamide (11)

A mixture of 2-(4-(trifluoromethyl)phenyl-5-(2,3-dihydro-4-iodo-2,2-dimethyl-5-nitrobenzofuran-7-yl)-1,3,4-oxadiazole (**10**) (10 g) and iron powder (2 g) in methanol was stirred at 25–30°C. To this mixture conc. HCl (10 mL) was added dropwise. After completion of reaction, the reaction mixture was basified by saturated $NaHCO_3$ solution, filtered through celite bed and extracted using dichloromethane. The organic layer was dried over anhydrous sodium sulphate and filtered. The solvent was removed under reduced pressure to afford 7-[5-(4-(trifluoromethyl)phenyl]-1,3,4-oxadiazol-2-yl)-2,3-dihydro-4-iodo-2, 2-dimethylbenzofuran-5-yl)amine (8 g). This was then dissolved in THF (50 mL) at 0°C and mixed with triethylamine (10 mL). The reaction mixture was further stirred at 0°C for 20 min, followed by pivolyl chloride (1.92 mL) and stirred for 2 h. After completion of reaction, the reaction mixture was extracted by EtOAC, the organic phase dried over anhydrous sodium sulfate, then the solvent was removed under reduced pressure to afford product which was recrystallized by diethyl ether to give **11** as a yellow solid (8.45 g), yield = 76.88%, mp = 162–163°C; ^{1}H NMR (300 MHz, DMSO-d_6): δ 1.27 (s, 9H), 1.56 (s, 6H), 3.10 (s, 2H), 8.02 (d, *J* = 8.4 Hz, 2H), 8.30 (d, *J* = 7.8 Hz, 2H), 9.12 (s, 1H), 9.35 (s, 1H); M.F. = $C_{24}O_3N_3IF_3H_{23}$ (MW = 584) *m/z* 585.92 $(M+H)^+$.

4.1.2 | General procedure for the synthesis of 12a–j

To a solution of *N*-{7-[5-(4-trifluoromethylphenyl]-1,3,4-oxadiazol-2-yl}-2,3-dihydro-4-iodo-2,2-dimethyl benzofuran-5-yl)pivalamide (**11**) (150 mg, 0.256 mmol) in DMSO, tetrabutyl ammonium fluoride monohydrate (TBAF) (217 mg, 0.767 mmol), acetylene derivatives (0.307 mmol) and bis-dichlorotriphenylphospine palladium(II) $PdCl_2(PPh_3)_2$ (3.5 mg, 0.0051 mmol) was added. The reaction mixture was stirred at 80°C for 3–4 h. After completion of reaction (as indicated by TLC), reaction mixture was quenched in water and extracted in ethyl acetate. The solvent was removed under reduced pressure and collected crude products were purified by column chromatography (4% methanol/dichloromethane).

N-(2,2-Dimethyl-4-(phenylethynyl)-7-(5-(4-(trifluoromethyl)-phenyl)-1,3,4-oxadiazol-2-yl)-2,3-dihydrobenzofuran-5-yl)-pivalamide (12a)

Faint yellow solid (yield = 85%), mp = 188–189°C. IR (KBr, cm^{-1}) ν 3426 (NH amide), 2969 CH), 2211 (C≡C), 1678 (C═O amide), 1543 (aromatic carbon), 1324 (C═N), 1170, 1127 (C-O), 1494 (C-F); ^{1}H NMR (300 MHz, DMSO-d_6): δ 1.28 (s, 9H), 1.58 (s, 6H), 3.28 (s, 2H), 7.48 (d, *J* = 7.6 Hz, 3H), 7.55 (d, *J* = 7.6 Hz, 2H), 7.92 (s, 1H), 8.03 (d, *J* = 7.8 Hz, 2H), 8.30 (d, *J* = 7.8 Hz, 2H), 9.15 (s, 1H, exchangeable with D_2O); ^{13}C NMR (125.7 MHz, $CDCl_3$): δ 27.8, 28.5, 40.2, 42.9, 88.4, 89.6, 90.7, 106.1, 117.6, 120.8, 126.1, 127.3, 127.5, 127.6, 128.7, 128.9, 129.7, 130.2, 131.7, 131.8, 132.0, 132.2, 135.9, 153.6, 162.9, 176.2; M.F. = $C_{32}O_3N_3F_3H_{28}$ (MW = 559.58) *m/z* 560.03 $(M+H)^+$.

N-(4-(Cyclohexylethynyl)-2,2-dimethyl-7-(5-(4-(trifluoromethyl)-phenyl)-1,3,4-oxadiazol-2-yl)-2,3-dihydrobenzofuran-5-yl)-pivalamide (12b)

White solid (yield = 82%) mp = 171–172°C. IR (KBr, cm^{-1}) ν 3382 (NH amide), 2930 CH), 2220 (C≡C), 1671 (C═O amide), 1519

(aromatic carbon), 1325 (C═N), 1169, 1118 (C-O), 1428 (C-F); ^{1}H NMR (300 MHz, DMSO-d_6): δ 1.26 (s, 9H), 1.32–1.24 (m, 4H), 1.48 (m, 2H), 1.54 (s, 6H), 1.68 (d, 2H), 1.84 (d, 2H), 2.71 (m, 1H), 3.12 (s, 2H), 8.01 (s, 1H), 8.01 (d, *J* = 8.1 Hz, 2H), 8.28 (d, *J* = 8.1 Hz, 2H), 8.83 (s, 1H, exchangeable with D_2O); ^{13}C NMR (125.7 MHz, $CDCl_3$): δ 22.2, 27.7, 27.8, 28.4, 28.5, 29.8, 30.8, 40.1, 42.8, 81.4, 90.4, 103.4, 105.4, 114.8, 117.1, 124.5, 126.1, 127.5, 127.6, 128.4, 131.3, 132.1, 153.4, 162.9, 176.5; M.F. = $C_{32}O_3N_3F_3H_{34}$ (MW = 565.26) *m/z* 566.03 $(M+H)^+$.

N-(4-(Cyclopentylethynyl)-2,2-dimethyl-7-(5-(4-(trifluoromethyl)phenyl)-1,3,4-oxadiazol-2-yl)-2,3-dihydrobenzofuran-5-yl)pivalamide (12c)

White solid; (yield = 80%) mp = 172–173°C. IR (KBr, cm^{-1}) ν 3382 (NH amide), 2930 CH), 2220 (C≡C), 1671 (C═O amide), 1519 (Ar-H), 1325 (C═N), 1169, 1118 (C-O), 1428 (C-F); ^{1}H NMR (300 MHz, DMSO-d_6): δ 1.23 (s, 9H), 1.54 (s, 6H), 1.54 (m, 4H), 1.92–1.60 (m, 2H), 2.45 (m, 4H), 3.14 (m, 1H), 3.33 (s, 2H), 7.57 (s, 1H), 8.02 (d, *J* = 8.4 Hz, 2H), 8.29 (d, *J* = 8.4 Hz, 2H), 9.15 (s, 1H, exchangeable with D_2O); ^{13}C NMR (125.7 MHz, $CDCl_3$): δ 27.8, 28.4, 28.5, 29.8, 35.1, 40.2, 43.0, 81.3, 88.0, 89.7, 106.7, 113.7, 120.7, 122.8, 126.1, 127.4, 130.9, 131.9, 132.5, 134.6, 135.1, 153.6, 165.3, 176.6; M.F. = $C_{31}O_3N_3F_3H_{32}$ (MW = 551.60) *m/z* 552.03 $(M+H)^+$.

N-(4-(Cyclopropylethynyl)-2,2-dimethyl-7-(5-(4-(trifluoromethyl)phenyl)-1,3,4-oxadiazol-2-yl)-2,3-dihydrobenzofuran-5-yl)pivalamide (12d)

White solid; (yield = 82%) mp = 176–177°C. IR (KBr, cm^{-1}) ν 3351 (NH amide), 2971 CH), 2220 (C≡C), 1660 (C═O amide), 1556 (Ar-H), 1324 (C═N), 1170, 1131 (C-O), 1462 (C-F); ^{1}H NMR (300 MHz, DMSO-d_6): δ 0.77 (d, 2H), 0.979 (d, 2H), 1.25 (s, 9H), 1.53 (m, 1H), 1.45 (s, 6H), 2.71 (m, 1H), 3.12 (s, 2H), 7.95 (s, 1H), 8.02 (d, *J* = 8.4 Hz, 2H), 8.28 (d, *J* = 8.4 Hz, 2H), 8.86 (s, 1H, exchangeable with D_2O); ^{13}C NMR (125.7 MHz, $CDCl_3$): δ 0.29, 9.2, 9.3, 28.2, 28.3, 40.0, 42.6, 68.9, 89.2, 90.2, 105.1, 106.3, 114.5, 116.9, 125.9, 126.0, 127.2, 127.4, 130.5, 131.9, 132.1, 153.2, 162.8, 176.3; M.F. = $C_{29}O_3N_3F_3H_{28}$ (MW = 523.55) *m/z* 524.00 $(M+H)^+$.

N-(2,2-Dimethyl-7-(5-(4-(trifluoromethyl)phenyl)-1,3,4-oxadiazol-2-yl)-4-((4-(trifluoromethyl)phenyl)ethynyl)-2,3-dihydrobenzofuran-5-yl)pivalamide (12e)

Off white solid; (yield = 75%) mp = 190–191°C. IR (KBr, cm^{-1}) ν 3354 (NH amide), 2965 (CH), 2346 (C≡C), 1678 (C═O amide), 1553 (aromatic carbon), 1325 (C═N), 1169, 1128 (C-O), 1460 (C-F); ^{1}H NMR (300 MHz, DMSO-d_6): δ 1.28 (s, 9H), 1.58 (s, 6H), 3.30 (s, 2H), 7.76 (d, *J* = 7.8 Hz, 2H), 7.85 (d, *J* = 7.8 Hz, 2H), 7.90 (s, 1H), 8.01 (d, *J* = 8.4 Hz, 2H), 8.31 (d, *J* = 8.4 Hz, 2H), 9.22 (s, 1H, exchangeable with D_2O); ^{13}C NMR (125.7 MHz, $CDCl_3$): δ 27.7, 29.8, 40.1, 42.8, 89.3, 90.4, 103.2, 105.3, 114.8, 117.1, 126.1, 126.2, 127.1, 127.3, 127.5, 127.5, 128.4, 130.7, 131.3, 132.0, 132.0, 153.4, 164.0, 176.5; M.F. = $C_{33}O_3N_3F_6H_{27}$ (MW = 627.58) *m/z* 628.12 $(M+H)^+$.

Methyl-5-chloro-2-((2,2-dimethyl-5-pivalamido-7-(5-(4-(trifluoromethyl)phenyl)-1,3,4-oxadiazol-2-yl)-2,3-dihydrobenzofuran-4-yl)ethynyl)benzoate (12f)

White solid; (yield = 78%) mp = 198–199°C. IR (KBr, cm^{-1}) ν 3347 (NH amide), 2965 CH), 2220 (C≡C), 1660 (C═O amide), 1738 (ester), 1554 (aromatic carbon), 1324 (C═N), 1170, 1128 (C-O), 1435 (C-F); ^{1}H NMR (300 MHz, DMSO-d_6): δ 1.28 (s, 9H), 1.58 (s, 6H), 3.33 (s, 3H), 3.89 (s, 3H), 7.72 (s, 1H), 7.89 (s, 1H), 7.99 (d, *J* = 8.4 Hz, 2H), 8.01 (s, 1H), 8.31 (d, *J* = 8.4 Hz, 2H), 9.23 (s, 1H, exchangeable with D_2O); ^{13}C NMR (125.7 MHz, $CDCl_3$): δ 28.5, 29.8, 40.2, 43.0, 52.9, 89.7, 98.0, 106.7, 113.7, 118.2, 120.7, 122.8, 126.2, 127.4, 127.6, 130.9, 131.9, 132.0, 132.5, 134.6, 134.9, 135.1, 153.6, 165.3, 176.6; M.F. = $C_{34}O_5N_3ClF_3H_{29}$ (MW = 652.06) *m/z* 652.09 (M+).

N-(4-((2,2-Dimethyl-4-oxochroman-8-yl)ethynyl)-2,2-dimethyl-7-(5-(4-(trifluoromethyl)phenyl)-1,3,4-oxadiazol-2-yl)-2,3-dihydrobenzofuran-5-yl)pivalamide (12g)

Yellow solid; (yield = 70%) mp = 212–213°C. IR (KBr, cm^{-1}) ν 3347 (NH amide), 2965 CH), 2220 (C≡C), 1660 (C═O, amide), 1738 (ester), 1554 (aromatic carbon), 1324 (C═N), 1170, 1128 (C-O), 1435 (C-F); ^{1}H NMR (300 MHz, DMSO-d_6): δ 1.48–1.30 (s, 21H), 2.70 (s, 2H), 3.3 (s, 2H), 7.33 (d, *J* = 7.5 Hz, 1H), 7.82 (d, *J* = 7.8 Hz, 2H), 7.88 (d, *J* = 7.5 Hz, 3H), 8.29 (d, *J* = 7.8 Hz, 3H); ^{13}C NMR (125.7 MHz, $CDCl_3$): δ 27.8, 27.9, 28.5, 28.6, 40.2, 42.9, 43.0, 48.9, 84.9, 88.4, 89.6, 90.7, 96.6, 106.1, 117.6, 120.8, 126.1, 127.3, 127.5, 127.6, 128.7, 128.9, 129.7, 130.2, 131.7, 131.8, 132.0, 132.2, 135.9, 153.5, 162.9, 176.6, 196.6, M.F. = $C_{37}O_5N_3F_3H_{34}$ (MW = 657.68) *m/z* 658.17 $(M+H)^+$.

N-(2,2-Dimethyl-4-(pent-1-ynyl)-7-(5-(4-(trifluoromethyl)-phenyl)-1,3,4-oxadiazol-2-yl)-2,3-dihydrobenzofuran-5-yl)-pivalamide (12h)

White solid; (yield = 75%) mp = 126–127°C. IR (KBr, cm^{-1}) ν 3322 (NH amide), 2964 (CH), 2228 (C≡C), 1671 (C═O amide), 1550 (aromatic carbon), 1324 (C═N), 1168, 1129 (C-O), 1428 (C-F); ^{1}H NMR (300 MHz, DMSO-d_6): δ 1.13 (t, 3H), 1.37 (s, 9H), 1.51 (m, 2H), 1.62 (s, 6H), 2.52 (t, 2H), 3.13 (s, 2H), 7.78 (d, *J* = 7.8 Hz, 2H), 8.19 (s, 1H), 8.30 (d, *J* = 7.8 Hz, 2H), 8.87 (s, 1H); ^{13}C NMR (125.7 MHz, $CDCl_3$): δ 13.7, 21.8, 22.3, 27.7, 28.4, 40.1, 42.8, 89.3, 90.4, 101.4, 105.3, 114.8, 117.1, 126.2, 127.1, 127.5, 128.4, 130.7, 131.3, 132.0, 153.4, 164.0, 176.5; M.F. = $C_{29}O_3N_3F_3H_{30}$ (MW = 525.56) *m/z* 526.69 $(M+H)^+$.

N-(4-(Hex-1-ynyl)-2,2-dimethyl-7-(5-(4-(trifluoromethyl)-phenyl)-1,3,4-oxadiazol-2-yl)-2,3-dihydrobenzofuran-5-yl)-pivalamide (12i)

White solid; (yield = 70%) mp = 132–133°C. IR (KBr, cm^{-1}) ν 3413 (NH amide), 2959 (CH), 2217 (C≡C), 1682 (C═O, amide), 1547 (aromatic carbon), 1324 (C═N), 1163, 1126 (C-O), 1424 (C-F); ^{1}H NMR (300 MHz, DMSO-d_6): δ 1.13 (t, 3H), 1.37 (s, 9H), 1.62 (m, 10H), 2.59 (t, 2H), 3.12 (s, 2H), 7.78 (d, *J* = 7.8 Hz, 2H), 8.18 (s, 1H), 8.30 (d, *J* = 7.8 Hz, 2H), 8.87 (s, 1H); ^{13}C NMR (125.7 MHz, $CDCl_3$): δ = 13.7, 19.5, 22.2, 27.7, 28.4, 30.9, 40.1, 42.8, 89.4, 90.4, 101.6, 105.4, 114.8, 117.1, 124.5, 126.1, 127.4, 128.4, 130.7, 131.3, 133.3, 153.4, 163.0, 176.5; M.F. = $C_{30}O_3N_3F_3H_{32}$ (MW = 539.59) *m/z* 541.16 $(M+H)^+$.

N-(4-(3-Hydroxyprop-1-ynyl)-2,2-dimethyl-7-(5-(4-(trifluoromethyl)phenyl)-1,3,4-oxadiazol-2-yl)-2,3-dihydrobenzofuran-5-yl)pivalamide (12j)

Off-white solid; (yield = 75%) mp = 182–183°C. IR (KBr, cm^{-1}) v 3405 (NH amide and OH alcohol), 2971 (CH), 2226 (C≡C), 1660 (C═O amide), 1502 (aromatic carbon), 1325 (C═N), 1165, 1125 (C-O), 1440 (C-F); ^{1}H NMR (300 MHz, DMSO-d_6): δ 1.26 (s, 9H), 1.54 (s, 6H), 3.15 (s, 2H), 4.38 (d, 2H), 5.44 (t, 1H, exchangeable with D_2O), 7.62 (s, 1H), 8.03 (d, J = 7.8 Hz, 2H), 8.28 (d, J = 7.8 Hz, 2H), 8.83 (s, 1H, exchangeable with D_2O); ^{13}C NMR (125.7 MHz, $CDCl_3$): δ 27.7, 28.4, 40.1, 42.7, 51.5, 88.1, 89.7, 90.8, 109.6, 117.9, 121.0, 124.8, 126.1, 127.1, 128.6, 130.9, 132.1, 132.3, 153.5, 164.5, 176.9; M.F. = $C_{27}O_4N_3F_3H_{26}$ (MW = 513.51) m/z 514.24 $(M+H)^+$.

4.2 | Statistical analysis

All the experiments were performed in triplicates and repeated at least twice and the data has been presented as mean SD (±). The % inhibition was calculated with the OriginPro 8 program (Origin Lab, Inc.) and the associated $GI_{50}/IC_{50}/GI_{90}/IC_{90}$ values have been noted.

ACKNOWLEDGMENT

Authors are thankful to Principal, PVP College, Pravaranagar, for providing necessary laboratory facilities and National Chemical Laboratory (NCL), Pune, for providing biological screening facilities.

CONFLICT OF INTEREST

The authors declare no conflict of interest.

ORCID

Somnath Gholap http://orcid.org/0000-0002-0883-3889

REFERENCES

[1] D. G. Russell, C. E. Barry, J. E. Flynn, *Science* **2010**, *328*, 852.
[2] C. Dye, B. G. Williams, *Science* **2010**, *328*, 856.
[3] J. P. Euzeby, List of bacterial names with standing in nomenclature-Genus *Mycobacterium* 2006. Available online at: http://www.bacterio.cict.fr/m/mycobacterium.html
[4] Z. Ma, A. M. Ginsberg, M. Spigelman, *Global Alliance for TB Drug Development*. New York, NY, USA, Elsevier Ltd. **2007**. *7*, pp. 699–730.
[5] M. M. Sankar, J. Singh, S. C. A. Diana, S. Singh, *Tuberculosis* **2013**, *93*, 75.
[6] N. R. Gandhi, P. Nunn, K. Dhedai, H. S. Schaaf, M. Zignol, S. D. Van, P. Jensen, J. Bayona, *Lancet* **2010**, *375*, 1830.
[7] A. A. Valayati, M. R. Masjedi, P. Farnia, P. Tabarsi, J. Ghanavi, A. H. Ziazarifi, S. E. Hoffner, *Chest* **2009**, *136*, 420.
[8] D. B. Young, M. Perkins, K. Duncan, C. E. Barry, *Clin. Invest*. **2008**, *118*, 1255.
[9] N. Anand, K. Upadhyaya, R. P. Tripathi, *Chem. Biol. Interface* **2015**, *5*, 84.
[10] A. Zumla, M. Raviglione, R. Hafner, C. F. Reyan, *Engl. J. Med*. **2013**, *368*, 745.
[11] C. R. W. Guimaraes, D. L. Boger, W. L. Jorgensen, *J. Am. Chem. Soc*. **2005**, *127*, 17377.
[12] J. Bostrom, A. Hogner, A. Llinas, E. Wellner, A. T. Plowright, *J. Med. Chem*. **2012**, *55*, 1817.
[13] E. J. North, M. S. Scherman, D. F. Bruhn, J. S. Scarborough, M. M. Maddox, V. Jones, A. Gregorzewicz, L. Yang, T. Hess, C. Morisseau, M. Jackson, M. R. Mcneil, R. E. Lee, *Bioorg. Med. Chem*. **2013**, *2*, 2587.
[14] N. D. James, J. W. Zibotentan, *Drugs Future* **2009**, *34*, 624.
[15] A. A. El-Emam, O. A. Al-Deeb, M. Al-Omar, J. Lehmann, *Bioorg. Med. Chem*. **2004**, *12*, 5107.
[16] P. R. Kagthara, N. S. Shah, R. K. Joshi, H. H. Parekh, *Ind. J. Chem*. **1999**, *38B*, 572.
[17] M. Akhter, A. Husain, B. B. Azad, M. Ajmal, *Eur. J. Med. Chem*. **2009**, *44*, 2372.
[18] P. C. Unangast, G. P. Shrum, D. T. Conner, C. D. Dyer, D. J. Schrier, *J. Med. Chem*. **1992**, *35*, 3691.
[19] M. S. Y. Khan, R. M. Khan, S. Drabu, *Indian J. Hetrocycl. Chem*. **2001**, *11*, 119.
[20] A. A. Farghaly, A. A. Bekhit, J. Y. Park, *Arch. Pharm. (Weinheim)* **2000**, *333*, 53.
[21] D. W. Robertson, W. B. Lacefield, W. Bloomquist, W. Pfeifer, R. L. Simon, M. L. Cohen, *J. Med. Chem*. **1992**, *35*, 310.
[22] J. Cheng, P. M. Giguere, W. Lv, B. L. Roth, A. P. Kozikowski, *Tetrahedron Lett*. **2015**, *56*, 3420.
[23] C. Sukbok, H. Y. Soon, L. P. Ho, *Tetrahedron Lett*. **2001**, *42*, 4833.
[24] B. E. Omar, H. Christopher, T. Queguiner, M. Francis, *Chem. Commun*. **2010**, *46*, 7043.
[25] S. S. Gholap, *Eur. J. Med. Chem*. **2016**, *110*, 13.
[26] S. S. Gholap, B. P. Bandgar, H. V. Chavan, V. D. Dhakane, U. P. Deshmukh, *C. R. Chim*. **2014**, *17*, 431.
[27] S. S. Gholap, U. P. Deshmukh, *Iranian J. Catal*. **2013**, *3*, 171.
[28] S. S. Gholap, V. D. Dhakane, S. S. Gholap, *Jordan J. Chem*. **2012**, *7* (3), 279.
[29] S. S. Gholap, N. Gunjal, *Arabian J. Chem*. **2017**, *10*, S2750.
[30] S. S. Gholap, N. Gunjal, *Iranian J. Catal*. **2016**, *8*, 147.
[31] S. R. Ugale, S. S. Gholap, *Chem. Pap*. **2017**, *71* (12), 2435.
[32] S. Helga, K. Andreas, *Tetrahedron Lett*. **2013**, *54*, 753.
[33] H. Rongjun, B. Yunpeng, Y. Zhi-Hong, Z. Zhang-Yin, *Med. Chem. Commun*. **2014**, *10*, 1496.
[34] S. Ursula, B. Frederic, Q. Anna, B. Christian, *J. Org. Chem*. **2013**, *78*, 6890.
[35] R. Nicholas, Y. Cai-Guang, H. Chauan, *Synlett* **2006**, *8*, 1278.
[36] B. Richard, M. Hanniffy, C. Stephes, A. Burke, *J. Org. Chem*. **2008**, *73*, 1354.
[37] H. M. Antonic, W. Johan, L. Mats, *Synlett* **2004**, *13*, 2335.
[38] U. Singh, S. Akhtar, A. Mishra, D. Sarkar, *J. Microbiol. Methods* **2011**, *84*, 202.
[39] (a) A. Khan, S. Sarkar, D. A. Sarkar, J. Microbiol. Methods 2008, 73, 62; (b) S. Sarkar, D. Sarkar, *J. Biomol. Screen*. **2012**, *17*, 966.
[40] A. Chollet, L. Mourey, C. Lherbet, A. Delbot, S. Julien, M. Baltas, J. Bernadou, G. Pratviel, V. Bernardes-Génisson, L. Maveyraud, *J. Str. Biol*. **2015**, *190* (3), 328.
[41] R. C. Hartkoorn, B. Chandler, A. Owen, S. A. Ward, S. Bertel, D. J. Back, S. H. Khoo, *Tuberculosis* **2007**, *87*, 248.
[42] X. He, A. Alian, R. Stroud, P. R. Ortiz de Montellano, *J. Med. Chem*. **2006**, *49*, 6308.
[43] D. A. Rozwarski, C. Vilche, M. Sugantino, R. Bittman, J. C. Sacchettini, *J. Bio. Chem*. **1999**, *274*, 15582.
[44] S. R. Luckner, N. Liu, C. W. Ende, P. J. Tonge, C. A. Kisker, *J. Biol. Chem*. **2010**, *285*, 14330.
[45] Y. Huang, R. P. Hickey, J. L. Yeh, D. Liu, A. Dadak, L. H. Young, R. S. Johnson, F. J. Giordano, *FASEB J*. **2004**, *18*, 1138.
[46] M. B. Bhalerao, S. T. Dhumal, A. R. Deshmukh, L. U. Nawale, V. Khedkar, D. Sarkar, R. A. Mane, *Bioorg. Med. Chem. Lett*. **2017**, *27*, 288.

[47] N. C. Desai, H. Somani, A. Trivedi, K. Bhatt, L. Nawale, V. M. Khedkar, P. C. Jha, D. Sarkar, *Bioorg. Med. Chem. Lett*. **2016**, *26*, 1776.
[48] S. T. Dhumal, A. R. Deshmukh, M. R. Bhosle, V. M. Khedkar, L. U. Nawale, D. Sarkar, R. A. Mane, *Bioorg. Med. Chem. Lett*. **2016**, *26*, 3646.
[49] S. Zhang, Y. Luo, L.-Q. He, Z.-J. Liu, H.-L. Zhu, *Bioorg. Med. Chem*. **2013**, *21*, 3723.
[50] Y. Cheng, W. H. Prusoff, *Biochem. Pharmacol*. **1973**, *22*, 3099.
[51] D. Lagorce, O. Sperandio, H. Galons, M. A. Miteva, B. O. Villoutreix, *BMC Bioinformatic* **2008**, *9*, 396.
[52] C. A. Lipinski, F. Lombardo, B. W. Dominy, P. J. Feeney, *Adv. Drug. Deliv. Rev*. **2001**, *46*, 3.
[53] S. Boyer, I. Zamora, *J. Comp. Aid. Mol. Des*. **2002**, *16*, 403.
[54] L. Carlsson, O. Spjuth, S. Adams, R. Glen, S. Boyers, *BMC Bioinformatic* **2010**, *11*, 362.
[55] S. Boyer, C. H. Arnby, L. Carlsson, J. Smith, V. Stein, R. C. Glen, *J. Chem. Inf. Model*. **2007**, *47*, 583.
[56] R. C. Braga, V. M. Alves, C. M. Fraga, E. J. Barreiro, V. de Oliveira, C. H. Andrade, *J. Mol. Model*. **2012**, *18*, 2065.
[57] F. A. Kalam Khan, Z. Zaheer, J. N. Sangshetti, R. H. Patil, M. Farooqui, *Bioorg. Med. Chem. Lett*. **2017**, *27*, 567.

SUPPORTING INFORMATION

Additional Supporting Information may be found online in the supporting information tab for this article.

How to cite this article: Gholap S, Tambe M, Nawale L, Sarkar D, Sangshetti J, Damale M. Design, synthesis, and pharmacological evaluation of fluorinated azoles as anti-tubercular agents. *Arch Pharm Chem Life Sci*. 2017;1–14. https://doi.org/10.1002/ardp.201700294